Indian J. Phys. **75B** (1), 37–47 (2001)

I J P B
— an international journal

Hall effect with simultaneous thermal and mass diffusion on unsteady hydromagnetic flow near an accelerated vertical plate

M Acharya†, G C Dash‡ and L P Singh*

†Department of Physics, College of Basic Science and Humanities, O U A T., Bhubaneswar-751 003, India

‡Department of Mathematics, C.E.T., O.U.A.T., Bhubaneswar-751 003, India

*Department of Physics, Utkal University, Bhubaneswar-751 004, India

Received 31 August 2000, accepted 13 November 2000

Abstract The effect of Hall current with simultaneous thermal and mass diffusion on unsteady laminar hydromagnetic viscous incompressible and electrically conducting fluid past a uniformly accelerated vertical porous plate (electrically non conducting) embedded in a uniform transverse magnetic field with heat source is investigated on the assumption of small magnetic Reynolds number. The results are discussed with respect to hydro magnetic parameter (Mt), Hall parameter (m), the buoyancy ratio parameter (N), Suction or injection parameter (a), Schmidt number (Sc) and heat source parameter (s) for $Pr = 0.71$ with respect to air.

Keywords Natural convection, buoyancy ratio parameter, hall current, magnetic field parameter

PACS Nos. 44.30.+v, 47.15.Cb, 47.55.Mh

1. Introduction

Magnetohydrodynamics is currently undergoing a period of great enlargement and differentiation of subject matter. The interest in these new problems stems from their importance in liquid metals, electrolytes and ionized gases. The thermal physics of MHD processes and MHD mass transfer are of interest in power engineering and metallurgy. The boundary zone between hydraulics and thermal physics is the arena of many cross galvano and thermomagnetic effects. These phenomena are important in the study of semiconductor materials. In magnetohydrodynamics, serious attention has been given only to the transverse galvanomagnetic effect *i.e.*, Hall effect; crossed phenomena also occur in the interaction of heat and mass transfer and hydraulics and mass transfer processes. The problem of magnetohydrodynamic viscous flow with Hall current have been studied by several workers [1–11]. Hartmann [12] has obtained an exact solution of magnetohydrodynamical equations of viscous incompressible fluid. The results obtained by Hartmann are applicable to ohmic fluid having isotropic conductivity *i.e.* liquid metals. The mechanism of conduction in ionized gasses (low density) in presence of strong magnetic field is different from that in metallic substance. The electric current in ionized gas is usually carried by electrons which undergo successive collisons with other charged or neutral particles. In case of ionized gas, the current is not proportional to applied potential except when the electric field is very weak. When the electric field is strong, the conductivity of ionized gas is affected by the magnetic field. Due to gyration and drift of charged particles, the conductivity parallel to the electric field is reduced and current is induced in the direction normal to both electric and magnetic fields. This phenomenon is known as Hall effect. The effect can be taken into account within the range of magnetohydrodynamical approximation.

Under the influence of electric and magnetic fields, dispersed particles begin to move relative to the supporting medium. This motion disrupts the equillibrium distribution of the particles in the stream. Moreover, the field can orient the particles, change the structure of the stream *etc.* All these factors cannot always be taken into account within the scope of pseudohomogenous approximation. This makes it necessary to develop hydraulics, thermal physics and mass transfer directly for two and multiphase systems.

†Corresponding Author

Thus the study of heat and mass transfer in case of incompressible electrical conducting media, must receive the same attention given to hydraulic and electrodynamic processes Sometimes the fluid flow is driven or modified by density differences caused by temperature, chemical composition differences and gradients and materials or phase constitution. However flow arising from differences in concentration or material constitution alone and in conjunction with temperature effects, causes buoyancy effects. Hall effects impose some restrictions on the regime of applicability of many solutions in which partially ionized gases are analysed using continuum MHD. Therefore, it is interesting to investigate flows resulting from buoyancy forces which arise from a combination of temperature and species concentration effects of comparable magnitude with Hall effect

In this paper, the effect of Hall current on the unsteady free convection flow of a viscous incompressible and electrically conducting fluid resulting from the simultaneous thermal and mass diffusion along an accelerated vertical porous plate (electrically non conducting) subjected to a constant magnetic field perpendicular to the plate, has been investigated The effect of heat source has also been studied In order to obtain similar solution, we consider $v(t)\alpha t^{-1/2}$ and solutions are obtained for a small time value. Expressions for velocity and skin frictions are obtained in case of small magnetic numbers and heat source parameter The numerical results for the velocity distributions (primary and secondary), skin friction, temperature distributions, concentration distributions are presented graphically and those of skin frictions are given in tabular form The present discussion is confined to the case when Pr (Prandtl number) = 0.71 (for air) and Sc (Schmidt number) is other than unity

2. Basic mathematical aspects

Consider the unsteady flow of a viscous incompressible and electrically conducting fluid past an infinite vertical porous plate located at $y = 0$ moving uniformly in its own plane with a velocity $U_0 t$ (where U_0 is constant velocity and t is the time variable) in presence of transverse magnetic field and heat source. The fluid in contact with the plate occupies the region $y > 0$ and is supposed to be at rest initially and at infinite at $t > 0$. The x axis is chosen along the plate in upward direction while y axis is chosen normal to it and away from the plate surface All the properties of the fluid are assumed to be constant, except the body force term causing buoyancy effect. The effect of Hall current gives rise to a force in the z direction which induces a cross flow in that direction. Thus the flow become three dimensional. The equation governing the flow of fluid together with Maxwell's electromagnetic equations are as follows [5] :

Continuity equation

$$\nabla . V = 0, \tag{1}$$

Momentum equation

$$\frac{\partial V}{\partial t} + (V.\nabla)V = -\frac{1}{\rho}\nabla p + \nu\nabla^2 V + g\beta(T - T_\infty) + g\beta^*(C - C_\infty) + \frac{1}{\rho}(J \times B), \tag{2}$$

Energy equation

$$\frac{\partial T}{\partial t} + (V.\nabla)T = K\nabla^2 T, \tag{3}$$

Generalised Ohm's law

$$J = \sigma(E + V \times B) - \frac{\sigma}{en_e}(J \times B - \nabla P_e), \tag{4}$$

Maxwell's equations

$$\nabla \times H = J, \ \nabla \times E = 0, \ \nabla . B = 0, \tag{5}$$

where V is the velocity vector, t the time, B the magnetic induction vector, E the electric field vector, J the Current density vector, P the pressure of the fluid, P_e the electron pressure, ρ the density of the fluid, σ ($= e^2 n_e \tau_e / m_e$) the electrical conductivity, e the electron charge, n_e the electron number density, τ_e the electron collision time, m_e the mass of an electron. If the magnetic Reynold number is small, induced magnetic field is neglected in comparison with the applied magnetic field, so that $B = (0, B_0, 0)$ [13]. The equation of conservation of electric charge $\nabla . J = 0$ gives J_y = constant, where $J = (J_x, J_y, J_z)$. As the plate is non conducting, $J_y = 0$ at the plate and hence zero everywhere. Considering the magnetic field strength to be very large, the corresponding generalised Ohm's law in the absence of electric field takes the following form

$$J + \frac{\omega_e \tau_e}{B_0}(J \times B) = \sigma\left(V \times B + \frac{\nabla p_e}{en_e}\right) \tag{6}$$

where $\omega_e (= eB_0 / m_e)$ is the electron frequency. For weekly ionised gases the electron pressure gradient and ionship effects (arising out of imperfect coupling between ions and neutrals) are neglected. Then equation (6) reduces to

$$J_x = \frac{\sigma B_0}{1 + m^2}(mu - w) \tag{7}$$

and

$$J_z = \frac{\sigma B_0}{1 + m^2}(u + mw) \tag{8}$$

where u, v and w are x, y and z components of velocity vector respectively, m is the Hall parameter defined by $m = \omega_e \tau_e$.

As the plate is infinite in length, all the variables in this problem are functions of y and t. Under this condition, Boussinesq approximation equations governing the flows are as follows :

Continuity equation

$$\frac{\partial v}{\partial y} = 0, \tag{9}$$

Momentum equation

$$\frac{\partial u}{\partial t}+v\frac{\partial u}{\partial y}=v\frac{\partial^2 u}{\partial y^2}-\frac{\sigma B_0^2}{\rho(1+m^2)}(u+mw)+g\beta\theta+g\beta^*C' \quad (10)$$

$$\frac{\partial w}{\partial t}+v\frac{\partial w}{\partial y}=v\frac{\partial^2 w}{\partial y^2}-\frac{\sigma B_0^2}{\rho(1+m^2)}(w-mu), \quad (11)$$

Energy equation

$$\frac{\partial \theta}{\partial t}+v\frac{\partial \theta}{\partial y}=\frac{v}{Pr}\frac{\partial^2 \theta}{\partial y^2}, \quad (12)$$

Equation of species concentration

$$\frac{\partial C'}{\partial t}+v\frac{\partial C'}{\partial y}=\frac{v}{Sc}\frac{\partial^2 C'}{\partial y^2} \quad (13)$$

where θ is the local temperature excess *i.e.* the difference between the local temperature and that at a very large distance from the plate, where temperature T is constant and equal to T_∞ ($\theta = T - T_\infty$). Similarly $C' = C^* - C_\infty$, g the acceleration due to gravity, T is the temperature of fluid within the boundary layer, C' is the species concentration, β is the volumetric coefficient of thermal expansion, β^* the volumetric coefficient of thermal expansion with concentration, v is the kinematic viscosity, Pr ($= \mu C_p/k$) is the Prandtl number, μ the dynamic viscosity, Cp, the specific heat at constant pressure, k the thermal conductivity, Sc ($= v/D$) the Schmidt number and D is the chemical molecular diffusivity s is the heat generation parameter. In equation (12) the term due to viscous dissipation is neglected and in eq (13) the term due chemical reaction is assumed to be absent.

The initial and boundary condition for the present problem are given as follows :

$$u(y,t) = w(y,t) = 0,\ \theta(y,t) = 0,\ C'(y,t) = 0,$$

everywhere for $t \le 0$;

$$u(0,t) = U_0 t,\ w(0,t) = 0,\ \theta(0,t) = \theta_0 t^{\alpha+1},$$
$$C'(0,t) = C_0 t^{\alpha+1} \text{ at } t > 0$$
$$u(\infty,t) = w(\infty,t) = 0,\ \theta(\infty,t) = 0,\ C'(\infty,t) = 0$$
$$\text{for } t > 0 \quad (14)$$

where α is a positive integer, $\theta_0 (= T_w - T_\infty)$ and C_0 ($= C_w - C_\infty$) are constants.

From eq. (9) it follows that v is either constant or function of time a only. According to Hasimoto [14], similarity solutions of eqs. (10–13) with the boundary condition (14) exist only if we consider

$$v(t) = -at^{-1/2}, \quad (15)$$

where a is constant. For suction, $a > 0$, and for injection or blowing $a < 0$. It is noted that the solution is valid for small values of time variable. To find solutions of eq. (10) and (11), we expand the dependent variables in power of hydromagnetic parameter (Mt) as given below

$$u(\eta,t) = U_0 g\beta\theta_0 t^{\alpha+2}\sum_{i=0}^{\infty}(Mt)^i u_i(\eta),$$

$$w(\eta,t) = U_0 g\beta\theta_0 t^{\alpha+2}\sum_{i=0}^{\infty}(Mt)^i w_i(\eta), \quad (16)$$

where $M = \sigma B_0^2/\rho$ (magnetic field parameter) and $\eta = \frac{y}{2\sqrt{vt}}$ is the similarity variable.

Since eqs (12) and (13) are independent of above variables, therefore we seek solutions to (12) and (13) in the following form.

$$\theta = \theta_0 t^{\alpha+1} f(\eta) \quad (17)$$

$$C' = C_0 t^{\alpha+1} g(\eta). \quad (18)$$

Now substituting (17), (18) together with (15) and (16) into eqs (10–15) and equating coefficients of equal powers of (Mt), we obtain the following set of equations :

$$f'' + 2Prf'(\eta + a) - 4Pr(\alpha + s + 1)f = 0,$$
$$g'' + 2Scg'(\eta + a) - 4Sc(\alpha + 1)g = 0,$$
$$u_0'' + 2(\eta + a)u_0' - 4(\alpha + 2)u_0 = -4f - 4Ng,$$
$$u_1'' + 2(\eta + a)u_1' - 4(\alpha + 3)u_1 = \frac{4}{1+m^2}(u_0 + mw_0),$$
$$u_2'' + 2(\eta + a)u_2' - 4(\alpha + 4)u_2 = \frac{4}{1+m^2}(u_1 + mw_1),$$
$$w_0'' + 2(\eta + a)w_0' - 4(\alpha + 2)w_0 = 0,$$
$$w_1'' + 2(\eta + a)w_1' - 4(\alpha + 3)w_1 = \frac{4}{1+m^2}(w_0 - mu_0),$$
$$w_2'' + 2(\eta + a)w_2' - 4(\alpha + 4)w_2 = \frac{4}{1+m^2}(w_1 - mu_1), \quad (19)$$

where $N = \dfrac{g\beta^*(C_w - C_\infty)}{g\beta(T_w - T_\infty)}$ (20)

This quantity measures the relative importance of chemical and thermal diffusion in causing the density difference which drives the flow It is to be noted that N is zero for no species diffusion, infinite for no thermal diffusion, positive for both effects combining to drive the flow and negative for effects opposed [15].

The corresponding boundary conditions are as follows

$$u_0 = 1,\ u_i = 0,\ w_{i-1} = 0,$$
$$f = 1,\ g = 1, \text{ at } \eta = 0; \quad (21)$$
$$u_{i-1} = 0,\ w_{i-1} = 0 \quad \text{for } i = 1, 2, 3;$$
$$f \to 0,\ g \to 0 \text{ as } \eta \to \infty.$$

Now solving the coupled eq. (19) together with the boundary conditions (21) for $Pr \neq 1$ and $Sc \neq 1$, we obtain

$$f(\eta)=\frac{Hh_{2(\alpha+s+1)}\left(\sqrt{2Pr}(\eta+a)\right)}{Hh_{2(\alpha+s+1)}\left(\sqrt{2Pr}a\right)}, \tag{22}$$

$$g(\eta)=\frac{Hh_{2(\alpha+1)}\left(\sqrt{2Sc}(\eta+a)\right)}{Hh_{2(\alpha+1)}\left(\sqrt{2Sc}a\right)}, \tag{23}$$

$$u_0(\eta)=\frac{2NHh_{2\alpha+1}\left(\sqrt{2Sc}a\right)Hh_{2\alpha+4}\left(\sqrt{2}(\eta+a)\right)}{(Sc-1)Hh_{2\alpha+4}\left(\sqrt{2}a\right)Hh_{2\alpha+2}\left(\sqrt{2Sc}a\right)}$$

$$+\frac{Hh_{2\alpha+4}\left(\sqrt{2}(\eta+a)\right)}{Hh_{2\alpha+4}\left(\sqrt{2}a\right)}$$

$$+\frac{2Hh_{2\alpha+4}\left(\sqrt{2Pr}a\right)Hh_{2\alpha+4}\left(\sqrt{2}(\eta+a)\right)}{(Pr-1)Hh_{2\alpha+4}\left(\sqrt{2}a\right)Hh_{2\alpha+2}\left(\sqrt{2Pr}a\right)}$$

$$\frac{2Hh_{2\alpha+4}\left(\sqrt{2Pr}(\eta+a)\right)Hh_{2\alpha+2s+2}\left(\sqrt{2Pr}(\eta+a)\right)}{(Pr-1)Hh_{2\alpha+2s+2}\left(\sqrt{2Pr}a\right)Hh_{2\alpha+2}\left(\sqrt{2Pr}(\eta+a)\right)}$$

$$\frac{2NHh_{2\alpha+4}\left(\sqrt{2Sc}(\eta+a)\right)}{(Sc-1)Hh_{2\alpha+2}\left(\sqrt{2Sc}a\right)}, \tag{24}$$

$$u_1(\eta)=\frac{4Hh_{2\alpha+6}\left(\sqrt{2Pr}(\eta+a)\right)}{(Pr-1)^2(1+m^2)Hh_{2\alpha+4}\left(\sqrt{2}a\right)}$$

$$\frac{Hh_{2\alpha+4}\left(\sqrt{2}(\eta+a)\right)Hh_{2\alpha+4}\left(\sqrt{2Pr}a\right)}{Hh_{2\alpha+2}\left(\sqrt{2Pr}a\right)Hh_{2\alpha+4}\left(\sqrt{2Pr}(\eta+a)\right)}$$

$$\frac{4Hh_{2\alpha+2s+2}\left(\sqrt{2Pr}(\eta+a)\right)}{(Pr-1)^2(1+m^2)Hh_{2\alpha+2s+2}\left(\sqrt{2Pr}a\right)}$$

$$\frac{Hh_{2\alpha+6}\left(\sqrt{2Pr}(\eta+a)\right)}{Hh_{2\alpha+2}\left(\sqrt{2Pr}(\eta+a)\right)}$$

$$\frac{4NHh_{2\alpha+6}\left(\sqrt{2Sc}(\eta+a)\right)}{(Sc-1)^2(1+m^2)Hh_{2\alpha+4}\left(\sqrt{2}a\right)}$$

$$\frac{Hh_{2\alpha+4}\left(\sqrt{2Sc}a\right)Hh_{2\alpha+4}\left(\sqrt{2}(\eta+a)\right)}{Hh_{2\alpha+2}\left(\sqrt{2Sc}a\right)Hh_{2\alpha+4}\left(\sqrt{2Sc}(\eta+a)\right)}$$

$$\frac{4NHh_{2\alpha+6}\left(\sqrt{2Sc}(\eta+a)\right)}{(Sc-1)^2(1+m^2)Hh_{2\alpha+2}\left(\sqrt{2Sc}a\right)}, \tag{25}$$

$$u_2(\eta)=\frac{8(1-m^2)Hh_{2\alpha+4}\left(\sqrt{2}(\eta+a)\right)}{(1+m^2)^2(Pr-1)^3Hh_{2\alpha+4}\left(\sqrt{2}a\right)}$$

$$\frac{Hh_{2\alpha+4}\left(\sqrt{2Pr}a\right)Hh_{2\alpha+8}\left(\sqrt{2Pr}(\eta+a)\right)}{Hh_{2\alpha+2}\left(\sqrt{2Pr}a\right)Hh_{2\alpha+4}\left(\sqrt{2Pr}(\eta+a)\right)}$$

$$\frac{8(1-m^2)Hh_{2\alpha+8}\left(\sqrt{2Pr}(\eta+a)\right)}{(Pr-1)^3(1+m^2)^2Hh_{2\alpha+2s+2}\left(\sqrt{2Pr}a\right)}$$

$$\frac{Hh_{2\alpha+2s+2}\left(\sqrt{2Pr}(\eta+a)\right)}{Hh_{2\alpha+2}\left(\sqrt{2Pr}(\eta+a)\right)}$$

$$\frac{8N(1-m^2)Hh_{2\alpha+4}\left(\sqrt{2}(\eta+a)\right)}{(1+m^2)^2(Sc-1)^3Hh_{2\alpha+4}\left(\sqrt{2}a\right)}$$

$$\frac{Hh_{2\alpha+4}\left(\sqrt{2Sc}a\right)Hh_{2\alpha+8}\left(\sqrt{2Sc}(\eta+a)\right)}{Hh_{2\alpha+2}\left(\sqrt{2Sc}a\right)Hh_{2\alpha+4}\left(\sqrt{2Sc}(\eta+a)\right)}$$

$$\frac{8N(1-m^2)Hh_{2\alpha+8}\left(\sqrt{2Sc}(\eta+a)\right)}{(1+m^2)^2(Sc-1)^3Hh_{2\alpha+2}\left(\sqrt{2Sc}a\right)}, \tag{26}$$

$$w_1(\eta)=-\frac{4mHh_{2\alpha+4}\left(\sqrt{2Pr}a\right)Hh_{2\alpha+4}\left(\sqrt{2}(\eta+a)\right)}{(1+m^2)(Pr-1)^2Hh_{2\alpha+4}\left(\sqrt{2}a\right)}$$

$$\frac{Hh_{2\alpha+6}\left(\sqrt{2Pr}(\eta+a)\right)}{Hh_{2\alpha+2}\left(\sqrt{2Pr}a\right)Hh_{2\alpha+4}\left(\sqrt{2Pr}(\eta+a)\right)}$$

$$\frac{4mHh_{2\alpha+2s+2}\left(\sqrt{2Pr}(\eta+a)\right)}{(1+m^2)(Pr-1)^2Hh_{2\alpha+2s+2}\left(\sqrt{2Pr}a\right)}$$

$$\frac{Hh_{2\alpha+6}\left(\sqrt{2Pr}(\eta+a)\right)}{Hh_{2\alpha+2}\left(\sqrt{2Pr}(\eta+a)\right)}$$

$$\frac{4mNHh_{2\alpha+4}\left(\sqrt{2Sc}a\right)Hh_{2\alpha+4}\left(\sqrt{2}(\eta+a)\right)}{(1+m^2)(Sc-1)^2Hh_{2\alpha+4}\left(\sqrt{2Sc}(\eta+a)\right)}$$

$$Hh_{2\alpha+6}\left(\sqrt{2Sc}(\eta+a)\right)$$
$$Hh_{2\alpha+4}\left(\sqrt{2}a\right)Hh_{2\alpha+2}\left(\sqrt{2Sc}a\right.$$

$$+\frac{4mNHh_{2\alpha+6}\left(\sqrt{2Sc}(\eta+a)\right)}{(1+m^2)(Sc-1)^2Hh_{2\alpha+2}\left(\sqrt{2Sc}a\right)}, \tag{27}$$

$$w_2(\eta)=-\frac{16mHh_{2\alpha+4}\left(\sqrt{2Pr}a\right)Hh_{2\alpha+4}\left(\sqrt{2}(\eta+a)\right)}{(1+m^2)^2(Pr-1)^3Hh_{2\alpha+4}\left(\sqrt{2}a\right)}$$

$$\frac{Hh_{2\alpha+8}\left(\sqrt{2Pr}(\eta+a)\right)}{Hh_{2\alpha+2}\left(\sqrt{2Pr}a\right)Hh_{2\alpha+4}\left(\sqrt{2Pr}(\eta+a)\right)}$$

$$+\frac{16mHh_{2\alpha+2s+2}\left(\sqrt{2Pr}(\eta+a)\right)}{(1+m^2)^2(Pr-1)^3Hh_{2\alpha+2s+2}\left(\sqrt{2Pr}a\right)}$$

$$\frac{Hh_{2\alpha+8}\left(\sqrt{2Pr}(\eta+a)\right)}{Hh_{2\alpha+2}\left(\sqrt{2Pr}(\eta+a)\right)}$$

$$\frac{16mNHh_{2a+4}\left(\sqrt{2Sc}a\right)Hh_{2a+4}\left(\sqrt{2}(\eta+a)\right)}{(1+m^2)(Sc-1)^3\,Hh_{2a+4}\left(\sqrt{2}a\right)}$$

$$\frac{Hh_{2a+8}\left(\sqrt{2Sc}(\eta+a)\right)}{Hh_{2a+2}\left(\sqrt{2Sc}a\right)Hh_{2a+4}\left(\sqrt{2Sc}(\eta+a)\right)}$$

$$+\frac{16mNHh_{2a+8}\left(\sqrt{2Sc}(\eta+a)\right)}{(1+m^2)^2(Sc-1)^3\,Hh_{2a+2}\left(\sqrt{2Sc}a\right)}, \qquad (28)$$

where the function $Hh_n(z)$ is defined by

$$Hh_n(z)=\int_z^\infty \frac{(s-z)^n}{n!}\exp\left(-\frac{S^2}{2}\right)ds. \qquad (29)$$

All other properties of this function have been discussed by Jeffreys and Jeffreys [16]. Relations (16) together with (19), (21-29) give the required equations for primary and secondary velocity components u and w respectively. During the numerical calculations of the velocity functions, the value of Pr is chosen to be 0.71 which represents air at 20°C. The values of Schmidt number Sc are chosen such that they represent the diffusing chemical species of most common interest in air (for example in air due to presence of H_2, CO_2, H_2O and NH_3, the values of Sc are 0.22, 0.94, 0.60 and 0.78 [17]). The values of buoyancy ratio parameter chosen to be 2, 1 0, –0.5, –1 and –2, covering a wide range for discussion. For weakly ionized fluid, the value of Hall parameter m is less than unity [3].

3. Results and discussion

Considering the different values of physical parameters the primary and secondary velocity profiles are shown in Figures 1–6 Figures 7, 8 present the x and z component of skin friction. Temperature and concentration profiles are shown in Figures 9 and 10 respectively.

In Figure 1, the broken curves represent the effect of injection or blowing whereas the effect of suction is represented by solid curves. It is observed that the primary velocity u decreases and secondary velocity w increases near the plate very rapidly due to the effect of suction velocity. However, secondary velocity decreases as we go away from the plate. For stronger heat source, the primary velocity of the fluid adjacent to the wall exceeds the wall velocity both for suction and injection. In Figure 2, solid curves represent velocity components in presence of foreign species such as H_2, H_2O, NH_3 and CO_2 for suction ($a > 0$) and broken curves represent primary and secondary velocity components in presence of foreign species for injection ($a < 0$). Primary velocity decreases from certain value on the plate whereas secondary velocity increases near the plate. Comparative study of the curve reveals that velocity of fluid increases at each point with decrease in Sc (Lighter particles) for primary velocity. The reversal flow occur in case of secondary velocity component due to CO_2 (Sc = 0.94).

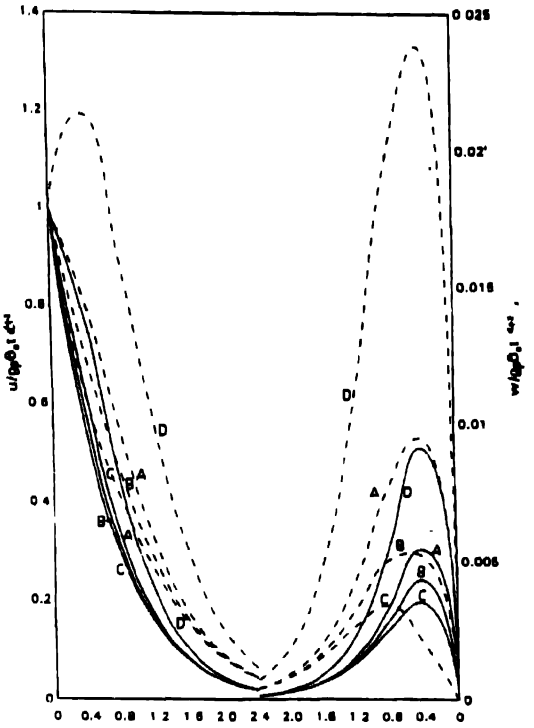

Figure 1. Velocity profiles against η for $\alpha = 0$, $Pr = 0.71$, $Sc = 0.22$, $N = 2.0$, $Mt = 0.2$, $m = 0.2$, $a = +0.5$ — $a = 0.5$ ---- $a = -0.5$ values of s for curve A = 0, B = 0.5, C = 1.0, D = – 1.0.

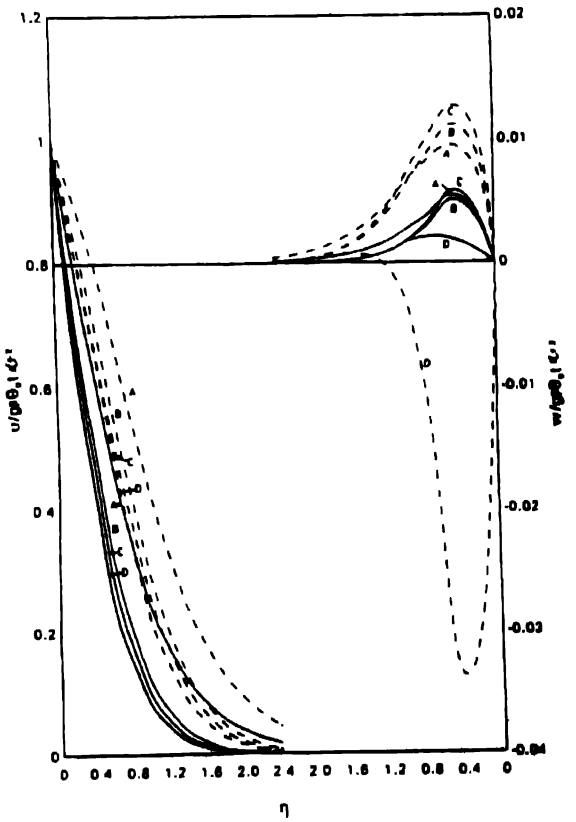

Figure 2. Velocity profiles against η for $\alpha = 0$, $Pr = 0.71$, $N = 2$, $Mt = 0.2$, $m = 0.2$, $a = \pm 0.5$, $s = 0$, ---- $a < 0$ – $a > 0$ values of Sc for curve A = 0.22, B = 0.6, C = 0.78, D = 0.94.

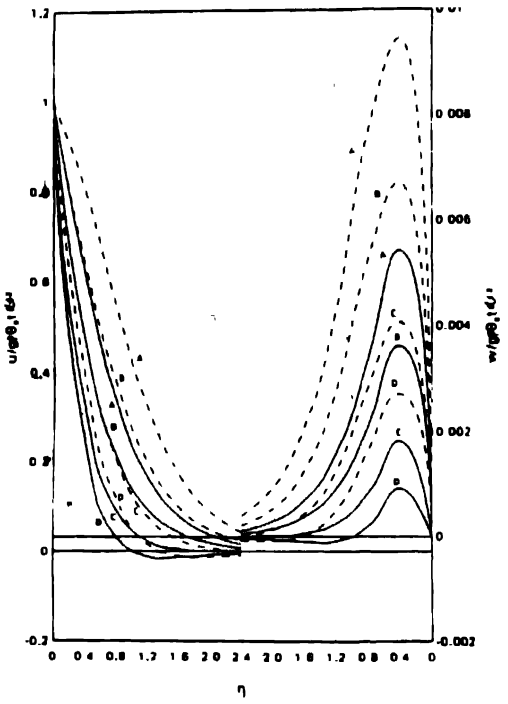

Figure 3. Velocity profiles against η for $\alpha = 0$, $s = 0$, $Pr = 0.71$, $Sc = 0.22$, $Mt = 0.2$, $m = 0.2$, $a = \pm 0.5$, — $a > 0$ ---- $a < 0$ values of N for curve A = 2.0, B = 1.0, C = 0.0, D = −0.5.

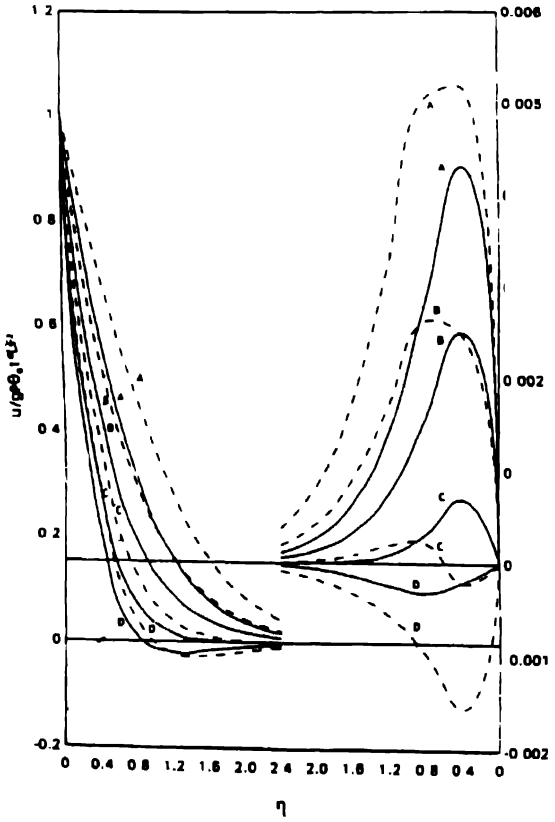

Figure 4. Velocity profiles against η for $\alpha = 0$, $s = 0.5$, $Pr = 0.71$, $Sc = 0.22$, $Mt = 0.2$, $m = 0.2$, $a = \pm 0.5$, — $a > 0$ ---- $a < 0$ values of N for curve A = 2.0, B = 1.0, C = 0.0, D = −0.5.

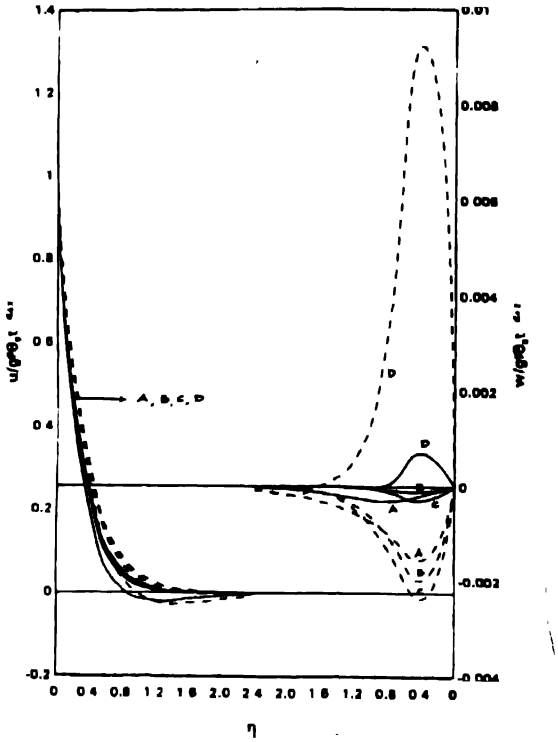

Figure 5. Velocity profiles against η for $\alpha = 0.0$, $s = 0.5$, $Pr = 0.71$, $N = 0.5$, $a = \pm 0.5$, — $a > 0$ ---- $a < 0$, $Mt = 0.2$, $m = 0.2$. Values of Sc for curve A = 0.22, B = 0.60, C = 0.78, D = 0.94

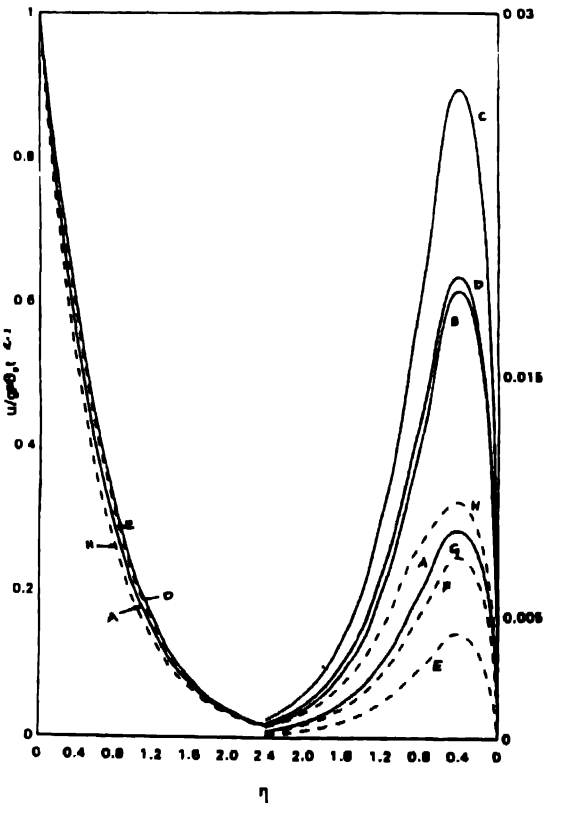

Figure 6. Velocity profiles against η for $\alpha = 0.0$, $Pr = 0.71$, $S = 0.5$, $Sc = 0.22$, $N = 2.0$, $a = 0.5$, $m = 1.0$, — $Mt = 0.5$ for different values of m. Curve A = 0.2, B = 0.5, C = 1.0, D = 3.0. ---- $m = 0.2$ for different values of Mt. Curve E = 0.2, F = 0.4, G = 0.5, H = 1.0.

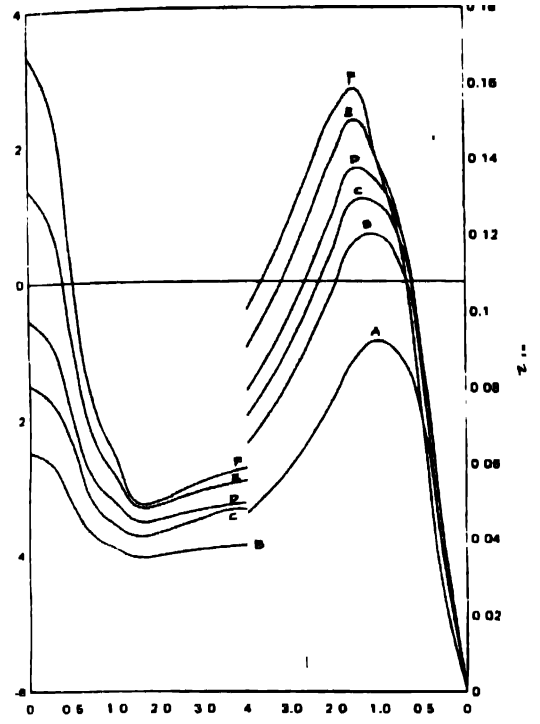

Figure 7(a). x and z components of skin friction against Hall parameter (m). $\alpha = 1.0$, $s = 0.5$, $Pr = 0.71$, $Sc = 0.22$, $N = 2.0$, $a = 0.5$. Values of Mt for curve A = 0.2, B = 0.4, C = 0.5, D = 0.6, E = 0.8, F = 1.0.

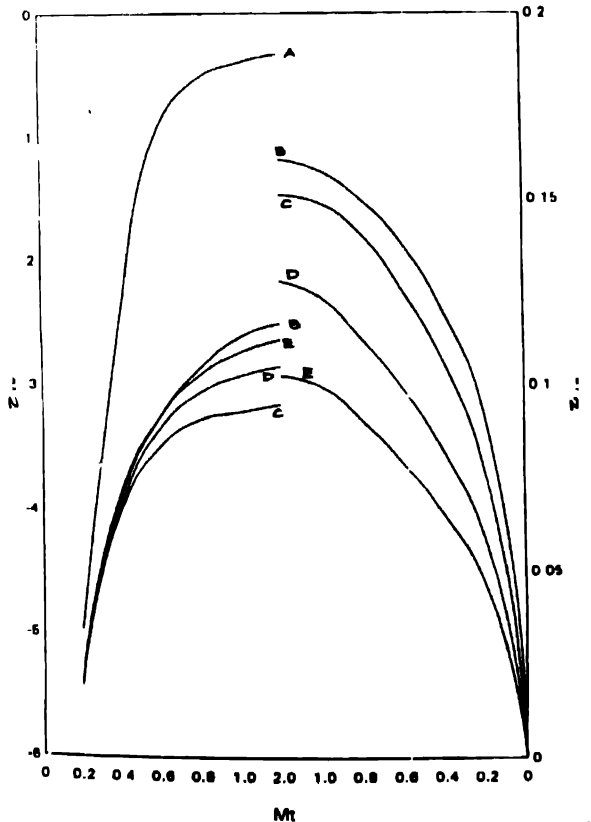

Figure 7(b). x and z components of skin friction against hydromagnetic parameter (Mt). $\alpha = 1.0$, $s = 0.5$, $Pr = 0.71$, $Sc = 0.22$, $N = 2.0$, $a = 0.5$. Values of m for curve A = 0.0, B = 1.0, C = 2.0, D = 3.0, E = 4.0

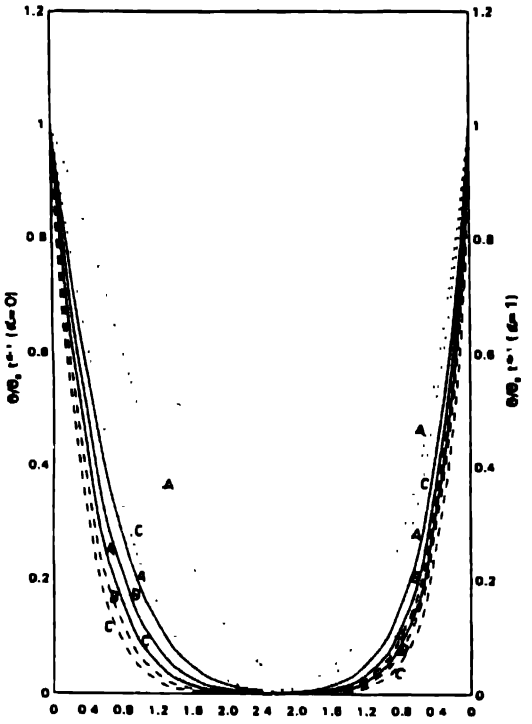

Figure 8. Temperature profiles against η for $Pr = 0.71$, — $s = 0$, —— $s = 1$ $s = -1$. Values of a for curve A = 0.5, B = 0.0, C = 0.5.

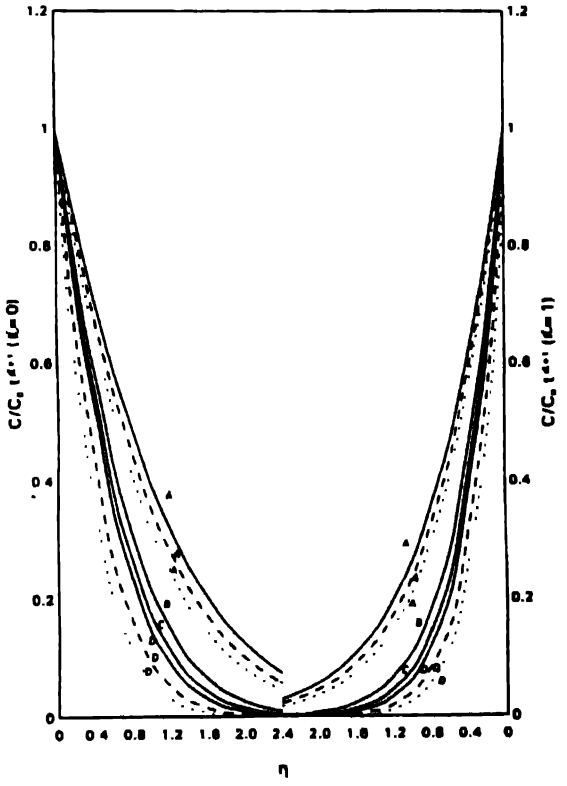

Figure 9. Species concentration profiles against η. Values of Sc for curve A = 0.22, B = 0.6, C = 0.78, D = 0.94, a = −0.5 — a = 0.0 — - a = 0.5 .....

Figure 3 (for $s = 0$) and Figure 4 (for $s = 0.5$) exhibit the effect of buoyancy ratio parameter over the flow field. The discussion has been carried out for $N = 0$ representing no species diffusion, $N > 0$ for both thermal and chemical diffusion combining to drive the flow and $N < 0$ representing the chemical and thermal effects as opposed to each other. For positive values of N, the magnitude of primary and secondary velocity components are more compared to $N = 0$ and $N < 0$. Comparing the curves of Figures 3 and 4, we conclude that in presence of heat source, the parameter magnitude of both primary and secondary velocity components decreases. The reversal flow occur in the cases of $N = -0.5$. This results from a very complicated interaction of the two buoyancy effects through velocity on the diffusion mechanism.

For aiding effects, decreasing Schmidt number increase the velocity level and its extent (Figure 2). For opposed effects, velocities are much lower and less for decreasing Schmidt number (Figure 5). Another interesting result is the large distortion of velocity field caused by decreasing values of N ($N = -0.5$). Negative values of velocity are predicted in the outer boundary region for smaller value of Sc for negative N. This results from the incoming flow first experiencing the negative buoyancy effect of the thicker species diffusion layer. The flow is eventually drawn upward by the combined action of thermally caused buoyancy and the shear that results therefrom.

The magnitude of primary velocity component decreases in presence of both heat source parameter and negative buoyancy parameter and the decrease is more for lighter particles. (Figure 5). Reversal effect is observed for CO_2 in case of secondary velocity component.

The dependence of primary and secondary velocities on hydromagnetic parameter Mt (broken curves) and Hall parameter m (solid curves) are shown in Figure 6. Flow along x axis tends to disappear, while the induced flow along z axis develops with increasing hydromagnetic parameter (Mt). The x component of velocity is modified and is monotonically decelerated due to an accelerating force which acts in the direction parallel to x axis. Thickening of primary velocity layer is observed with increasing Hall parameter. The induced flow along the z axis begins to develop as m increases from zero and form a maximum profile at $m = 1.0$ (weakly ionized gas). For a large value of m ($m > 1$) the flow tends to disappear. The maximum point of secondary velocity profile tends to shift away from the flat plate as the Hall parameter increases.

Temperature distribution :

Figure 8 shows the temperature distribution with respect to different values of transpiration parameter for $a > 0$, $a < 0$ (porous wall) and $a = 0$ (solid surface) and heat source parameter. An increase in the value of transpiration parameter indicates thinning of thermal boundary layer at all points of the flow field from the maximum value attained at the wall. The heat source brings about a temperature increase throughout the entire boundary layer. For stronger source the temperature of the fluid adjacent to the wall may exceed the wall temperature.

Concentration distribution :

Figure 9 shows the concentration distribution for the transpiration parameter $a = -0.5$, $a = 0.5$ (porous wall) and $a = 0$ (solid surface) in the presence of different diffusing species such as H_2, H_2O, NH_3 and CO_2 ($Sc = 0.22, 0.60, 0.78$ and 0.94). The concentration at all points in the flow field decreases for the uniformly heated plate. A comparative study of curves in the above figure shows a decrease in concentration at all points with an increase in Schmidt number (heavier particles) from the maximum value attained at the wall. To be precise, thinning effect is observed for heavier particles and finally suction parameter reduces the species concentration while injection parameter increases it.

It is also important to know the effect of physical parameters Sc, N, s, a, Mt and m on skin friction from these relations.

$$\tau_{xw} = \frac{1}{2\sqrt{Mt}}\left(\frac{\partial u}{\partial \eta}\right)_{\eta=0} \tag{30}$$

and

$$\tau_{zw} = \frac{1}{2\sqrt{Mt}}\left(\frac{\partial w}{\partial \eta}\right)_{\eta=0}, \tag{31}$$

where τ_{xw} and τ_{zw} are respectively the x and z component of skin friction with

$$\left(\frac{\partial u}{\partial \eta}\right)_{\eta=0} = -\frac{2\sqrt{2}\,Hh_{2a+4}\left(\sqrt{2Pr}a\right)Hh_{2a+3}\left(\sqrt{2}a\right)}{(Pr-1)Hh_{2a+4}\left(\sqrt{2}a\right)Hh_{2a+2}\left(\sqrt{2Pr}a\right)}$$

$$-\frac{2\sqrt{2}N\,Hh_{2a+4}\left(\sqrt{2Sc}a\right)Hh_{2a+3}\left(\sqrt{2}a\right)}{(Sc-1)Hh_{2a+4}\left(\sqrt{2}a\right)Hh_{2a+2}\left(\sqrt{2Sc}a\right)}$$

$$+\frac{2\sqrt{2Pr}\,Hh_{2a+2s+1}\left(\sqrt{2Pr}a\right)Hh_{2a+3}\left(\sqrt{2Pr}a\right)}{(Pr-1)Hh_{2a+2s+2}\left(\sqrt{2Pr}a\right)Hh_{2a+1}\left(\sqrt{2Pr}a\right)}$$

$$+\frac{2N\sqrt{2Sc}\,Hh_{2a+3}\left(\sqrt{2Sc}a\right)}{(Sc-1)Hh_{2a+2}\left(\sqrt{2Sc}a\right)} - \frac{\sqrt{2}\,Hh_{2a+3}\left(\sqrt{2}a\right)}{Hh_{2a+4}\left(\sqrt{2}a\right)}$$

$$+(Mt)\ -\frac{4\sqrt{2}\,Hh_{2a+4}\left(\sqrt{2Pr}a\right)}{(Pr-1)^2(1+m^2)Hh_{2a+4}\left(\sqrt{2}a\right)}$$

$$\frac{Hh_{2a+3}\left(\sqrt{2}a\right)Hh_{2a+5}\left(\sqrt{2Pr}a\right)}{Hh_{2a+2}\left(\sqrt{2Pr}a\right)Hh_{2a+3}\left(\sqrt{2Pr}a\right)}$$

$$+\frac{4\sqrt{2Pr}\,Hh_{2a+5}\left(\sqrt{2Pr}a\right)Hh_{2a+2s+1}\left(\sqrt{2Pr}a\right)}{(Pr-1)^2(1+m^2)Hh_{2a+1}\left(\sqrt{2Pr}a\right)Hh_{2a+2s+2}\left(\sqrt{2Pr}a\right)}$$

$$-\frac{4N\sqrt{2}Hh_{2a+5}(\sqrt{2Sc}a)}{(Sc-1)^2(1+m^2)Hh_{2a+4}(\sqrt{2}a)}$$

$$\frac{Hh_{2a+4}(\sqrt{2Sc}a)Hh_{2a+3}(\sqrt{2}a)}{Hh_{2a+2}(\sqrt{2Sc}a)Hh_{2a+3}(\sqrt{2Sc}a)}$$

$$-\frac{4N\sqrt{2Sc}Hh_{2a+5}(\sqrt{2Sc}a)}{(Sc-1)^2(1+m^2)Hh_{2a+2}(\sqrt{2Sc}a)}$$

$$+(Mt)\frac{-8\sqrt{2}(1-m^2)Hh_{2a+3}(\sqrt{2}a)}{(1+m^2)^2(Pr-1)^3Hh_{2a+4}(\sqrt{2}a)}$$

$$\frac{Hh_{2a+4}(\sqrt{2Pr}a)Hh_{2a+7}(\sqrt{2Pr}a)}{Hh_{2a+2}(\sqrt{2Pr}a)Hh_{2a+3}(\sqrt{2Pr}a)}$$

$$+\frac{8(1-m^2)\sqrt{2Pr}Hh_{2a+7}(\sqrt{2Pr}a)Hh_{2a+2+1}(\sqrt{2Pr}a)}{(Pr-1)^3(1+m^2)^2Hh_{2a+1}(\sqrt{2Pr}a)Hh_{2a+2+2}(\sqrt{2Pr}a)}$$

$$-\frac{8N\sqrt{2}(1-m^2)Hh_{2a+3}(\sqrt{2}a)}{(1+m^2)^2(Sc-1)^3Hh_{2a+4}(\sqrt{2}a)}$$

$$\frac{Hh_{2a+4}(\sqrt{2Sc}a)Hh_{2a+7}(\sqrt{2Sc}a)}{Hh_{2a+2}(\sqrt{2Sc}a)Hh_{2a+3}(\sqrt{2Sc}a)}$$

$$\frac{8N(1-m^2)\sqrt{2Sc}Hh_{2a+7}(\sqrt{2Sc}a)}{(Sc-1)^3(1+m^2)^2Hh_{2a+2}(\sqrt{2Sc}a)} \quad (32)$$

and $$\left(\frac{\partial w}{\partial \eta}\right)_{\eta=0} = Mt\left[\frac{4m\sqrt{2}Hh_{2a+4}(\sqrt{2Pr}a)}{(1+m^2)(Pr-1)^2Hh_{2a+4}(\sqrt{2}a)}\right.$$

$$\frac{Hh_{2a+3}(\sqrt{2}a)Hh_{2a+5}(\sqrt{2Pr}a)}{Hh_{2a+2}(\sqrt{2Pr}a)Hh_{2a+3}(\sqrt{2Pr}a)}$$

$$\frac{4m\sqrt{2Pr}Hh_{2a+5}(\sqrt{2Pr}a)Hh_{2a+2+1}(\sqrt{2Pr}a)}{(1+m^2)(Pr-1)^2Hh_{2a+1}(\sqrt{2Pr}a)Hh_{2a+2+2}(\sqrt{2Pr}a)}$$

$$+\frac{4mN\sqrt{2}Hh_{2a+4}(\sqrt{2Sc}a)}{(1+m^2)(Sc-1)^2Hh_{2a+3}(\sqrt{2Sc}a)}$$

$$\frac{Hh_{2a+3}(\sqrt{2}a)Hh_{2a+5}(\sqrt{2Sc}a)}{Hh_{2a+4}(\sqrt{2}a)Hh_{2a+2}(\sqrt{2Sc}a)}$$

$$\frac{4mN\sqrt{2Sc}Hh_{2a+5}(\sqrt{2Sc}a)}{(1+m^2)(Sc-1)^2Hh_{2a+2}(\sqrt{2Sc}a)}$$

$$+(Mt)\frac{16m\sqrt{2}Hh_{2a+4}(\sqrt{2Pr}a)}{(1+m^2)(Pr-1)^3Hh_{2a+4}(\sqrt{2}a)}$$

$$\frac{Hh_{2a+3}(\sqrt{2}a)Hh_{2a+7}(\sqrt{2Pr}a)}{Hh_{2a+2}(\sqrt{2Pr}a)Hh_{2a+3}(\sqrt{2Pr}a)}$$

$$\frac{16m\sqrt{2Pr}Hh_{2a+7}(\sqrt{2Pr}a)Hh_{2a+2+1}(\sqrt{2Pr}a)}{(1+m^2)^2(Pr-1)^3Hh_{2a+1}(\sqrt{2Pr}a)Hh_{2a+2+2}(\sqrt{2Pr}a)}$$

$$+\frac{16mN\sqrt{2}Hh_{2a+4}(\sqrt{2Sc}a)}{(1+m^2)^2(Sc-1)^3Hh_{2a+4}(\sqrt{2}a)}$$

$$\frac{Hh_{2a+3}(\sqrt{2}a)Hh_{2a+7}(\sqrt{2Sc}a)}{Hh_{2a+2}(\sqrt{2Sc}a)Hh_{2a+3}(\sqrt{2Sc}a)}$$

$$\frac{16mN\sqrt{2Sc}Hh_{2a+7}(\sqrt{2Sc}a)}{(1+m^2)^2(Sc-1)^3Hh_{2a+2}(\sqrt{2Sc}a)} \quad (33)$$

It is evident from eqs. (30–33) that the components of skin friction are proportional to components of velocity gradient at the surface of the plate. Numerically, x and z components of skin friction are calculated using different values of physical parameters. As before, here also we restrict our discussion to P_r = 0.71. (Values of Prandtl number for air at 20°C). We may conclude that x and z components of skin friction decrease with increase in heat source parameter for both suction and injection (Table 1). The x component of skin friction decreases for diffusion of heavier particles both for suction and injection (except for CO_2) *i.e.* velocity gradient at the surface decreases more in presence of heavier particles than in lighter particles (Table 2). However, the z component of skin friction increases owing to increase in species concentration (except for CO_2).

Table 1. Numerical values of x and z components of skin friction for different values of s at Pr = 0.71 and Sc = 0.22

α	s	$u'(0)/g\beta\theta_0 t^{a+2}$		$w'(0)/g\beta\theta_0 t^{a+2}$	
		a = 0.5	a = −0.5	a = 0.5	a = −0.5
1	−1.0	−2.8320	−0.8040	0.0421	0.0589
	0.0	4.791	3.220	0.0392	0.0473
	0.5	5.028	3.657	0.0328	0.0297
	1.0	−5.251	4.056	0.0268	0.0136

Table 3 shows decrease in the x and z components of skin friction with decrease in buoyancy ratio parameter both for suction and injection in case of suddenly heated plate and uniformly heated plate. Physically this means that fluid velocity increases due to the combined action of chemical and thermal diffusion and velocity decreases when both effects oppose each other.

In order to study the effect of hydromagnetic parameter and Hall current on the skin friction, the coefficients of skin friction are plotted in Figure 7(a) and Figure 7(b). It is shown that x component of skin friction decreases monotonically up to m = 1.0 and then increases. On the other hand, the z component of skin friction has a maximum for a particular

Table 2. Numerical values of x and z component of skin friction for different values of Sc, at $Pr = 0.71$, $N = 2.0$

		Sc	$\tau'(0)/g\beta\theta_0 t^{a+2}$		$w'(0)/g\beta\theta_0 t^a$	
			$a = +0.5$	$a = -0.5$	$a = 0.5$	$a = -0.5$
0	-1.0	0.22	0.2681	2.4579	0.1036	0.2072
		0.60	-0.3477	2.0533	0.1104	0.2265
		0.78	-0.6123	1.7991	0.1210	0.2238
		0.94	-0.8334	2.9029	0.0521	-0.7366
0	-0.5	0.22	-0.2052	0.7809	0.0883	0.1250
		0.60	-0.8211	0.3763	0.0951	0.1443
		0.78	-1.0856	0.1221	0.1056	0.1416
		0.94	-1.3068	1.2259	-0.0674	-0.8088
0	0.0	0.22	-1.0995	0.3140	0.0592	0.0713
		0.60	-1.7154	-0.7186	0.0660	0.0906
		0.78	1.9800	-0.9728	0.0766	0.0879
		0.94	2.2011	0.1309	0.0964	-0.8725
0	0.5	0.22	-1.4002	-1.2631	0.0495	0.0248
		0.60	2.0161	1.6677	0.0563	0.0441
		0.78	-2.2806	-1.9219	0.0668	0.0414
		0.94	2.5018	-0.8181	-0.1062	-0.9190
0	1.0	0.22	-1.7344	2.0905	0.0386	-1.5722
		0.60	2.3503	-2.4951	0.0454	0.0035
		0.78	2.6149	2.7493	0.0560	0.0087
		0.94	2.8361	1.6456	-0.1171	-0.9596

value of m. Maximum value of skin friction tends to shift away from the plate as magnetic interaction parameter increases (Figure 7(a)). For small values of Mt, the maximum skin friction is obtained when value of m is close to unity, which is also predicted in the work by Naruse [18]. x and z components of skin friction increase sharply with increasing magnetic interaction parameter upto $Mt = 0.5$ and after that increases gradually.

In Table 4, x and z components of skin frictions are tabulated for reversal flow ($N = -0.5$). The x component of skin friction increases both for suction and injection with increase in species concentration, whereas z component decreases both for suction and injection with increase in species concentration (except for CO_2).

4. Conclusions

The above studies on unsteady flow of viscous incompressible conducting fluid past an accelerated vertical porous plate, with a heat source embedded in a uniform magnetic field in presence of foreign species leads to the following conclusions:

1. On increasing heat source parameter, the magnitude of both primary and secondary velocity increases. For stronger source, the velocity of the fluid adjacent to the wall exceeds the wall velocity both for suction and injection.
2. Primary velocity in case of both suction and injection increases for lighter particles and a reversal flow occurs in secondary velocity in case of foreign species CO_2 ($Sc = 0.94$).
3. Above development casts the multiple buoyancy mechanism in vertical flow into a convenient similarity form. Calculations indicate many complicated

Table 3. Numerical values of x and z components of skin friction for different values of N, the buoyancy ratio parameter at $Pr = 0.71$, $Sc = 0.22$.

α	S	N	$\tau'(0)/g\beta\theta_0 t^{a+2}$		$w'(0)/g\beta\theta_0 t^a$	
			$+0.5$	$a = -0.5$	$a = 0.5$	$a = -0.5$
0	-1.0	2	0.2681	2.4579	0.1036	0.2072
		1	-0.8576	1.5373	0.0860	0.1874
		0	-1.9833	0.6167	0.0684	0.1676
		-0.5	-2.5462	0.1565	0.0596	0.1576
0	0	2	-1.0995	-0.3140	0.0592	0.0713
		1	-2.2253	-1.234	0.0416	0.0515
		0	-3.3510	-2.155	0.0240	0.0317
		-0.5	-3.9139	-2.6155	0.0152	0.0217
	0.5	2	-1.4002	-1.2631	0.0495	0.0248
		1	-2.5259	-2.1837	0.0319	0.0050
		0	-3.6517	-3.1042	0.0143	-0.0148
		-0.5	-4.2145	-3.5645	0.0055	-0.0247
	1.0	2	-1.7344	-2.0905	0.0386	-0.0157
		1	-2.8602	-3.0111	0.0210	-0.0355
		0	-3.9859	-3.9317	0.0034	-0.0553
		-0.5	-4.5488	-4.3920	-0.0053	-0.0653
1	0	2	-4.7918	-3.2202	0.0392	0.0473
		1	-4.1953	-2.6731	0.0281	0.0350
		0	-3.5987	-2.1259	0.0170	0.0228
		-0.5	-3.3005	-1.852	0.0114	0.0166
	0.5	2	-5.0286	-3.6573	0.0328	0.0297
		1	-4.4321	-3.1102	0.0217	0.0174
		0	-3.8355	-2.5631	0.0106	0.0051
		-0.5	-3.5373	-2.2895	0.00505	-0.0009
	1.0	2	-5.2517	-4.0563	0.0268	0.0136
		1	-4.6551	-3.5092	0.0157	.0013
		0	-4.0551	-2.9621	0.0045	-.0109
		-0.5	-3.7603	-2.6885	-0.0009	-.0170
	-1	2	-4.3233	-2.1718	.0519	.0896
		1	-3.7268	-1.6247	.0407	.0773
		0	-3.1302	-1.0776	.0296	.0651
		-0.5	-2.8320	-0.8040	.0241	.0589

Table 4. Numerical values of x and z components of skin friction for reversal flows at $Pr = 0.71$ and $N = -0.5$.

a	s	Sc	$u'(0)/g\beta\theta_0 t^{a+2}$		$w'(0)/g\beta\theta_0 t^{a+2}$	
			$a = 0.5$	$a = -0.5$	$a = 0.5$	$a = -0.5$
0	0	0.22	−3.9139	−2.6155	0.0152	0.0217
		0.60	−3.7599	−2.5143	0.0135	0.0169
		0.78	−3.6938	−2.4508	0.0109	0.0176
		0.94	−3.6385	−2.4267	0.0542	0.2577
0	0.5	0.22	−4.2145	−3.5645	0.0055	−0.0247
		0.60	−4.0606	−3.4634	0.0038	−0.0295
		0.78	−3.9944	−3.3998	0.0011	−0.0288
		0.94	−3.9391	−3.6758	0.0444	0.2112
0	1.0	0.22	−4.5488	−4.3920	−0.0053	−0.0653
		0.60	−4.3948	−4.2908	−0.0070	−0.0701
		0.78	−4.3287	−4.2273	−0.0096	−0.0694
		0.94	−4.2734	−4.5032	0.0336	0.1706
1.0	0	0.22	−3.3005	−1.8524	0.01145	0.0166
		0.60	−2.6024	−1.0117	0.0098	0.0131
		0.78	−1.5397	0.2922	0.0072	0.0105
		0.94	4.5752	7.6967	0.0209	0.0870
1.0	0.5	0.22	−3.5373	−2.2895	0.0050	−0.0009
		0.60	−2.8392	−1.4488	0.0034	−0.0044
		0.78	−1.7765	−1.449	0.0084	−0.0070
		0.94	4.3384	7.2595	0.0145	0.0694
1.0	1.0	0.22	−3.7603	−2.6885	−0.0009	−0.0170
		0.60	−3.0623	−1.8479	−0.0025	−0.0205
		0.78	−1.9996	−0.5439	−0.0051	−0.0231
		0.94	4.1153	6.6860	0.0085	0.0533

interactions which arise in such flows including reversal flows. It is also observed that opposing effects greatly distort the velocity distribution.

4. Primary and secondary velocity increase with increase in Hall parameter and for large values of m the induced flow along z axis tends to disappear.
5. Flow along x axis tends to disappear while the induced flow along x axis develops with increasing hydromagnetic parameter.
6. The skin friction components τ_{xw} and τ_{zw} decrease with increase in heat source parameter both for suction and injection. For heavier particles, velocity gradient at the surface decreases so also the skin friction components. Suction leads to decrease in skin friction components while injection leads to increase in skin friction components. Velocity gradient is larger for the case of combined effects of chemical and thermal diffusion than for these effects opposing each other.
7. x and z components of skin friction increase with increase in hydromagnetic parameter Mt.
8. x component of skin friction decreases monotonically for moderate values of Hall parameter and for small values of Mt, maximum value of z component of skin friction is obtained when the value of m is closed to unity.
9. Heat source brings about temperature increase in the fluid layer and for stronger source, the temperature of fluid layer may exceed the wall temperature.

References

[1] H Sato *Phys. Soc. Jpn* **16** 427 (1961)

[2] T Yamanishi *17th Annual Meeting, Physical Society of Japan (Osaka)* **5** 29 (1962)

[3] G W Sutton and A Shrerman *Magneto Hydrodynamics* (Illinois: Evaston) (1961)

[4] M Katagiri *J. Phys. Soc. Jpn* **27** 1051 (1969)

[5] I Pop *J. Math. Phys. Sci* **5** 375 ((1971)

[6] M A Hossain *J. Phys. Soc. Jpn* **55** 2183 (1986)

[7] V M Soundalgekar and P W Wavre *Int. J. Heat Mass Transfer* **20** 1365 (1977)

[8] M A Hossain and R A Begum *ASME J. Heat Transfer* **106** 664 (1984)

[9] G Mandal *et al J. Phys. Soc. Jpn* **51** 2010 (1982)

[10] M A Hossain and RIMA Rashid *J. Phys. Soc. Jpn* **56** 97 (1987)

[11] M Acharya *et al J. Phys.* **D28** 2455 (1995)

[12] H Hartmann *kgl. Danske Videusk. Selsk. Mat-Fys* **15** 6 (1937)

[13] T G Cowling *Magneto Hydrodynamics* (New York: Wiley Interscience) (1957)

[14] H Hasimoto *J. Phys. Soc. Jpn* **12** 68 (1957)

[15] B Gebhart and L Pera *Int. J. Heat Mass Transfer* **14** 2025 (1971)

[16] H Jeffreys and B S Jeffreys *Methods of Mathematical Physics* (Cambridge: Cambridge University Press) 622 (1972)

[17] B Gebhart *Heat Transfer* (New York: McGraw Hill) (1965)

[18] H Naruse *Bulletin of Aero. Res. Inst., Univ. of Tokyo* **3** A-1 (in Japanese) (1963)